


ORIGINAL ARTICLE OPEN ACCESS

Kullback–Leibler Divergence-Based Fault Detection Scheme for 100% Inverter Interfaced Autonomous Microgrids

 Ali Mallahi^{1,2} | Iman Sadeghkhani^{1,2} 
¹Smart Microgrid Research Center, Najafabad Branch, Islamic Azad University, Najafabad, Iran | ²Department of Electrical Engineering, Najafabad Branch, Islamic Azad University, Najafabad, Iran

Correspondence: Iman Sadeghkhani (sadeghkhani@pel.iaun.ac.ir)

Received: 15 November 2024 | **Revised:** 14 February 2025 | **Accepted:** 10 March 2025

Keywords: differential protection | fault detection | inverter | Kullback–Leibler divergence | microgrid

ABSTRACT

The development of a dependable and secure protection system is critical for further integration of renewable energy sources into electrical energy systems. To address the bidirectional power flow and limited fault current contribution of 100% inverter-based microgrids, this article presents a differential fault detection scheme (DFDI) based on monitoring the line-end current signals using an intelligent electronic device. The difference in current waveforms of a faulty line is quantified using the Kullback–Leibler divergence similarity measure. The efficacy of the proposed scheme in detecting severe and non-severe fault conditions with various fault inception angles in the presence of measurement noise and nonlinear load for both radial and loop configurations is assessed on two benchmark microgrids. As verified by various simulation scenarios on the benchmark microgrids, the proposed DFDI detects various types of faults in different locations with fault resistance up to 100 Ω . Moreover, it demonstrates high immunity to harmonics and measurement noise up to 25 dB. The results confirm that the proposed method offers a reliable, efficient, and adaptive solution for fault detection in inverter-based microgrids.

1 | Introduction

The imperative to integrate renewable energy source (RES) units into modern power grids is driven by the urgent need to reduce carbon emissions and mitigate the impacts of climate change [1]. Traditional power generation, heavily dependent on fossil fuels, is a major contributor to greenhouse gas emissions, underscoring the need to transition to cleaner and sustainable energy sources. Micro-grids offer a strategic framework for incorporating RES units such as solar and wind [2, 3]. These modern energy systems can be seamlessly isolated from the main grid and operate in islanded mode, whether planned or in response to unforeseen disruptions, ensuring continuous power supply and system resilience [4].

Environmental-friendly autonomous microgrids face two major challenges from intermittent power generation and protection perspectives; where the latter is the focus of this article. Conventionally, the distribution systems are protected using overcurrent based protective devices. In the presence of the main power grid or synchronous generators, the microgrid feeder current significantly increases in the case of a fault condition. However, limiting the fault current contribution of electronically- interfaced RES units to protect their semiconductor switches reduces the sensitivity of overcurrent protective devices. On the other hand, the distributed supply of the microgrid loads makes the power flow bidirectional, challenging the selectivity of the protection system.

Two major alternative relaying principles for overcurrent relays are distance and differential protections. The former suffers

This is an open access article under the terms of the [Creative Commons Attribution](https://creativecommons.org/licenses/by/4.0/) License, which permits use, distribution and reproduction in any medium, provided the original work is properly cited.

© 2025 The Author(s). *Energy Science & Engineering* published by Society of Chemical Industry and John Wiley & Sons Ltd.

from the need for a potential transformer (PT) and the possibility of misidentification of the faulty section due to the presence of several branches in distribution systems. Although the application of the latter is usually restricted to power apparatus [5], the emergence of smart grids with advanced communication infrastructure makes differential protection a promising solution for smart microgrids. Based on the processed quantity, recently developed differential fault detection schemes can be categorized into voltage and current-based schemes. The absence of PT units in available distribution systems significantly increases the cost of implementation of a voltage-based differential fault detection scheme such as [6–9]. A protection scheme that calculates the phase angle differences of positive-sequence currents of both line ends is outlined in [10]. In [11], a deep neural network-based data-mining model is presented where the differential current phasor is used. However, it requires a training data set. The fault detection scheme of [12] is based on the calculation of the differential angle of positive-sequence superimposed currents. Tajani et al. [13] employs the discrete wavelet transform on the differential current. However, these current-only references do not evaluate the performance of their proposed schemes in the presence of Nonlinear loads. By assessing the similarity between instantaneous phase currents retrieved from line-end current signals, Saber et al. [14] protect the microgrid feeders. However, it is not effective for a microgrid line with unidirectional power flow. In [15], a superimposed current based differential protection scheme is introduced, utilizing Park's transformation to extract phasors, while the Teager–Kaiser energy operator is used in [16] to compute the energy difference between line-end current signals, thereby protecting micro-grid feeders. However, robustness to measurement noise and the presence of nonlinear loads are not assessed in these references. A differential fault detection scheme is introduced in [17] that processes the differential current and the frequency components obtained from the synchro-squeezing transform. However, it requires several thresholds. Liu et al. [18] proposed a microgrid line protection scheme by calculating the transient wavelet energy of the superimposed current. Injection of an off-nominal frequency through the inverter control is the basic tool of the scheme in [19] to determine the differential current frequency components. El-Sayed et al. [20] injected two interharmonic currents during fault conditions by the inverter control system. Using edge computing techniques, time-domain energy features are extracted from line-end currents in [21]. In [22], the directionality information of positive sequence current-based microgrid protection is presented. However, these references do not evaluate their scheme in the presence of nonlinear loads and capacitor switching. The difference in the current wave-shapes at both ends of a microgrid faulty line is the basic principle of short-time correlation transform-based fault detection scheme in [23]. However, it does not evaluated during capacitor and operating mode switchings.

To address the shortcomings of previous works, this article proposes a differential fault detection scheme using the current signals retrieved from both ends of a microgrid line. First, the fault-imposed components of the current signals are calculated by an intelligent electronic device (IED) as the protective device of the proposed scheme. Then, the dissimilarity of current waveforms due to different directions of fault-imposed current

signals at two ends of a faulty line is quantified using the Kullback–Leibler (KL) divergence. By using a single threshold and without the need for a training data set, the proposed fault detection scheme presents a promising performance in the presence of measurement noise and nonlinear loads. Also, it is effective for microgrid lines with both unidirectional and bidirectional power flows. Several studies have utilized the KL divergence for fault detection in various engineering systems, focusing on incipient faults and sensor anomalies rather than electrical fault detection in power networks [24–26]. Unlike these works, our study applies KL divergence within the context of short-circuit and ground fault detection in 100% inverter-based autonomous microgrids, addressing the unique challenges of low fault currents, bidirectional power flow, and microgrid topology variations.

2 | Proposed Methodology

The KL divergence is a powerful measure from information theory that quantifies the difference between two probability distributions. While KL divergence is traditionally used to compare distributions, in the proposed fault detection scheme, this measure is adopted to track changes in the characteristics of current waveforms, rather than comparing entire distributions directly. In inverter-based microgrids, fault conditions can result in low fault current magnitudes, bidirectional power flow, and the presence of nonlinear behaviors due to the inverter control strategies. These factors make traditional protection schemes, which rely on significant changes in current magnitude, less reliable. On the other hand, KL divergence is sensitive to subtle variations in the distribution of current signals over time. By interpreting current signals as discrete signal distributions, KL divergence can quantify even small deviations from expected signal patterns, which are often indicative of fault conditions. The ability of KL divergence to capture deviations in the overall statistical distribution of the current signal rather than focusing solely on isolated data points or magnitudes allows it to detect faults even when the changes are not large enough to trigger traditional fault detection mechanisms. Furthermore, KL divergence's application is robust to noise, which is a critical issue in inverter-based microgrids, where switching transients and harmonic distortion can impact current measurements. These features makes it a superior choice for fault detection in environments where traditional protection schemes may fail to provide the necessary sensitivity and reliability.

In the first step of the proposed scheme, the current signals are measured at both ends of the microgrid line. An IED is used to attenuate the noise and sample these signals. To enhance the generalization of the developed differential scheme, the sampled feeder current signal in phase j , i_j , is normalized as

$$i_j^{\text{pu}}(kT_s) = \frac{i_j(kT_s)}{I_b}, \quad (1)$$

where i_j^{pu} is the current signal in per-unit, and k and T_s are the sampling step and period respectively. Base current I_b is calculated by dividing the base power by the base voltage.

In the next step, the superimposed current is calculated by the IED. The superposition theory allows for the separation of fault-induced signals from the normal operating signals by analyzing the superimposed components [27]. By isolating these fault-imposed components, it becomes possible to identify and analyze disturbances caused by faults, thereby facilitating their discrimination from regular system behavior. By using the Delta filter, the super-imposed component of the current signal $i_j^{pu, SI}$ is calculated as [28]

$$i_j^{pu, SI}(kT_s) = i_j^{pu}(kT_s) - i_j^{pu}(kT_s - T_d), \quad (2)$$

where T_d is the Delta filter time delay. By choosing T_d as a coefficient of the signal period, this component is zero during normal operation while it significantly changes when a fault occurs. Also, it has current directionality information. The super-imposed current is monitored by using a moving data window as

$$\mathbf{I}_j(kT_s) = [i_j^{pu, SI}(kT_s - WT_s) \dots i_j^{pu, SI}(kT_s)], \quad (3)$$

where W is the length of the moving window. Each window is updated with the arrival of a new superimposed current sample, simultaneously discarding the oldest sample. It increases the fault detection speed. For a faulty line, the current increases in one end while it decreases in another end, resulting in a positive super-imposed current in one end and a negative superimposed current for another end. This dissimilarity between two current sets at both ends \mathbf{I}_{Mj} and \mathbf{I}_{Nj} is quantified by using the KL divergence as

$$D_{KL,j}(\mathbf{I}_{Mj} \parallel \mathbf{I}_{Nj}) = \sum_{q=1}^W \mathbf{I}_{Mj}(q) \times \log \frac{\mathbf{I}_{Mj}(q)}{\mathbf{I}_{Nj}(q)}. \quad (4)$$

where D_{KL} is the proposed differential fault detection index (DFDI). A disturbance is classified as a fault condition if $D_{KL} > \xi$, where ξ is the threshold of fault detection. The flow-chart of the proposed fault detection scheme is shown in Figure 1. This algorithm is implemented as a new differential logic in the IEDs of the microgrid.

2.1 | Parameter Selection

The sampling period is adopted as low as 0.83 ms (20 samples per cycle). As mentioned above, the time delay of the Delta filter should be a coefficient of the signal period; thus it is set to one cycle (20 samples). The length of the moving data window is set to half cycle (10 samples). Thus, the only adjustable parameter of the proposed scheme is ξ . Careful threshold selection is critical to ensure the reliable performance of the proposed protection scheme. Due to measurement and switching noises, the D_{KL} is not precisely zero under normal operating conditions. To ensure the robustness of the proposed fault detection scheme and prevent malfunctions under no-fault disturbances, the threshold ξ is determined based on an extensive set of simulated scenarios. These scenarios included normal operation, high fault resistances, various fault inception angles (FIAs), high levels of measurement noise, load variations, and RES switching events. The maximum value of the proposed

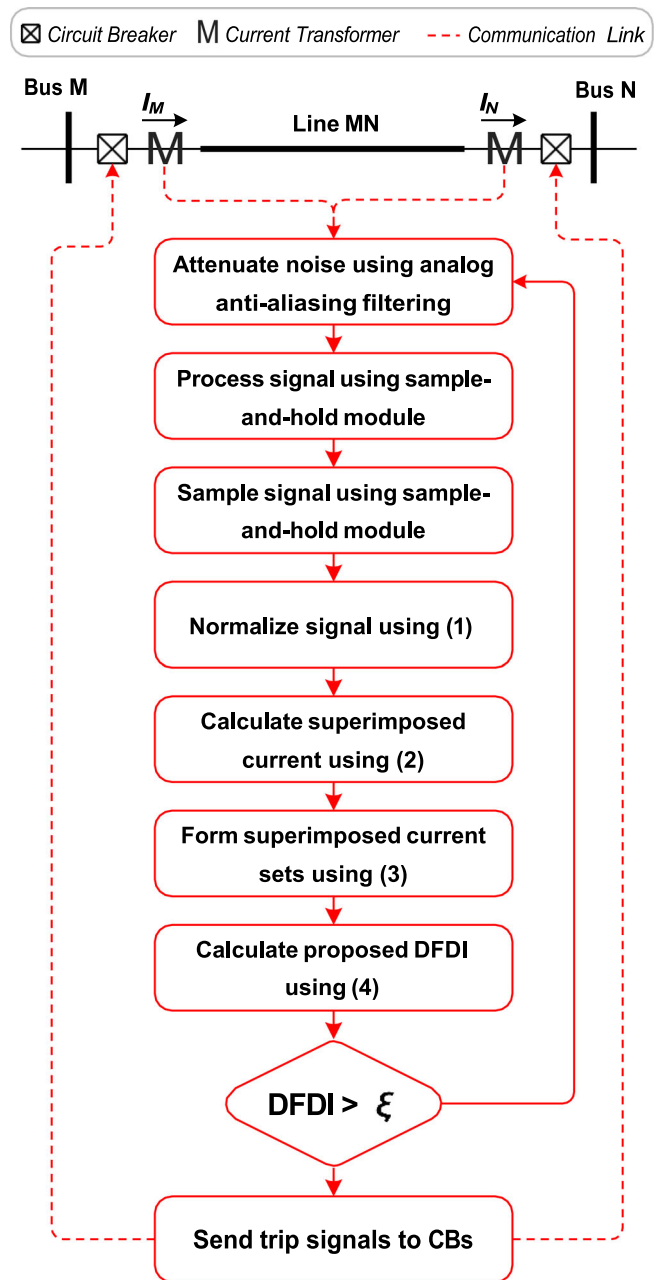


FIGURE 1 | Flowchart of the KL divergence-based differential fault detection scheme.

fault detection index is calculated during normal operation and no-fault scenarios in the presence of severe measurement noise. The simulation results show that the maximum value of D_{KL} during non-fault conditions is 2.5. To minimize the risk of false positives while ensuring reliable fault detection, a safety margin of 2 is applied, leading to a final threshold value of 5. The selection of this margin is based on ensuring that even under extreme non-fault disturbances, the KL divergence remains below the threshold, thereby avoiding triggering a false alarm while still maintaining sensitivity to actual faults.

2.2 | Impact of Communication Failure

Like all differential protection schemes, the proposed method relies on communication between IEDs at different line ends.

This inherent dependence on communication introduces a trade-off between protection sensitivity and reliability. While differential schemes offer highly selective and fast fault detection, communication failures can impact their operation. If a communication failure occurs, the IEDs would be unable to exchange current data, potentially leading to a failure in detecting faults. However, in practical implementations, several strategies can mitigate this issue. Redundant communication channels, such as dual-path fiber optics or wireless backup links, can enhance reliability.

2.3 | Impact of Communication Delay

As mentioned in [22] and [29], it is established that for transmission lines under 18 miles (approximately 29 km), the time required for signal transmission is less than 0.1 ms based on the speed of light, with only several additional microseconds needed for processing time. This is sufficient for most distribution systems, and as a result, there is no need for time-synchronized measurements from both ends of the line for short distribution lines. This is especially relevant in the context of inverter-based microgrids, where the lines are typically much shorter, and synchronization errors do not pose significant issues for differential protection. Given these short transmission distances, synchronization errors are practically negligible, making differential protection particularly effective in these settings. The short distances and minimal delays between measurement points mean that the protection scheme can operate without the complexities introduced by synchronization mismatches, which are typically a concern in longer transmission lines.

2.4 | Economic Feasibility

IEDs are advanced devices that combine fault detection, monitoring, and communication capabilities. These devices can provide a high level of functionality, such as real-time monitoring, fault diagnostics, and the ability to interface with a broader communication infrastructure. The initial cost of IEDs tends to be higher compared to traditional differential relays due to their more sophisticated hardware, software capabilities, and communication features. However, the additional functionalities offered by IEDs such as remote diagnostics, fault isolation, and real-time data analytics can significantly reduce operational costs, downtime, and maintenance needs, offering long-term savings.

Regarding the communication infrastructure, the proposed scheme leverages the existing infrastructure available in most smart grid networks. This significantly reduces the initial deployment cost, as it eliminates the need for dedicated, separate communication systems. Modern smart grids already incorporate fiber-optic cables, wireless communication, and other advanced communication technologies, which are capable of supporting the communication needs of the proposed fault detection scheme.

3 | Performance Evaluation

The single-line diagram of the study test microgrid is shown in Figure 2 which is simulated in the MATLAB/Simulink

environment. It is a section of the Canadian urban benchmark distribution system with few modifications [30]. The RES units are controlled using droop control and the injected current of their interface inverters is limited to twice the nominal current by using the hybrid reference frame limiting strategy [31]. The efficacy of the developed scheme is assessed by simulating several fault and no-fault scenarios. Table 1 presents the parameters of the study test system.

In the first scenario, a severe three-phase fault condition is simulated at Line 8–9 of the study test microgrid. Figure 3 presents the simulation results. The calculated D_{KL} is near zero for all healthy lines. Thus, the proposed scheme does not mal-operate for external faults. The calculated DFDI by the IED of Line 8–9 is 205.75, 213.12, and 194.79 for phases *a*, *b*, and *c*, respectively, which are much higher than the fault detection threshold of 5. Thus, this fault condition is detected by the proposed scheme and the trip command is sent to circuit breakers of the faulty line.

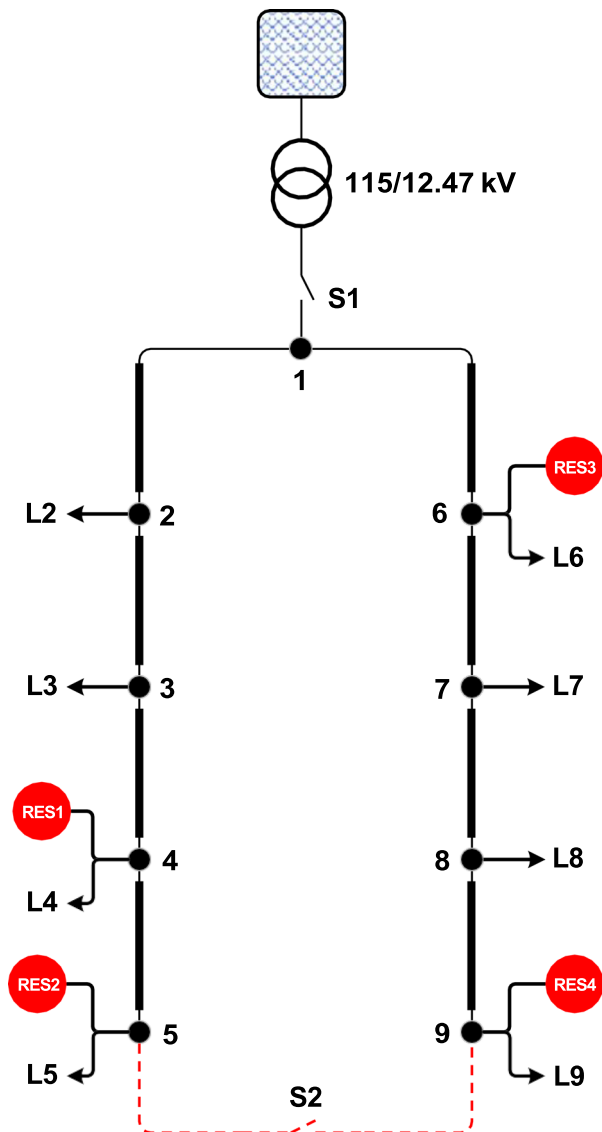


FIGURE 2 | Single-line diagram of the study test microgrid.

To evaluate the sensitivity of the proposed scheme, a single-phase to ground (*ag*) fault with fault resistance of $100\ \Omega$ is simulated at Line 2–3. Figure 4 presents the DFDI for all phases of study microgrid lines that The proposed DFDI for all phases of the study test microgrid is zero (near zero). For the faulty line, D_{KL} for the faulty phase increases to 9.67 while for healthy phases is zero, verifying the sensitivity of the proposed fault detection scheme. This fault condition is detected after about 8 ms by the IED of this line.

To assess the robustness of the proposed scheme to various FIAs, a two-phase fault (*bc*) with fault resistance of $5\ \Omega$ is simulated at Line 4–5 for three FIAs of 0° , 45° , and 90° . The simulation results are presented in Table 2. The calculated DFDI of healthy phases remains near zero for all FIAs while it increases significantly for faulty phases of the faulty line.

TABLE 1 | Parameters of the study test microgrid.

Parameter	Value
Nominal voltage and frequency	12.47 kV, 60 Hz
RES rating	2 MVA
RES interface transformer power and voltage	2 MVA, 12.47/0.6 kV
Line length	500 m
Positive sequence impedance	$0.511 + j0.366\ \Omega/\text{km}$
Positive sequence susceptance	$3.172\ \mu\text{S}/\text{km}$
Zero sequence impedance	$0.658 + j1.611\ \Omega/\text{km}$
Zero sequence susceptance	$1.28\ \mu\text{S}/\text{km}$
Load power and power factor	900 kVA, 0.9

Noise-contaminated signals may disrupt the operation of fault detection schemes. To evaluate the immunity of the proposed scheme, a single-phase to ground (*bg*) fault with fault resistance of $50\ \Omega$ is simulated at Line 3–4 and the retrieved signals are contaminated with the white Gaussian noise with the 25 dB signal-to-noise ratio. Table 3 shows that although the DFDI increases in healthy lines, these are lower than the fault detection threshold and this high measurement noise does not affect the selectivity of the proposed fault detection scheme.

Harmonic pollution is also one of the factors that threaten the effectiveness of fault detection schemes. To assess the efficacy of the proposed scheme for this case, load L3 is replaced by a non-linear load, modeled by a rectifier and parallel *RC* load. A solid three-phase fault is simulated at Line 1–2 and the simulation results are presented in Table 4. The presence of harmonics in feeder current signals does not result in malfunction of the proposed fault detection scheme and the fault is detected by the IED of faulty line.

Simultaneous faults are another fault conditions that are considered for evaluation of the proposed DFDI. A two-phase fault (*ac*) with fault resistance of $5\ \Omega$ at Line 3–4 is simulated simultaneously with a single-phase to ground fault (*bg*) with fault resistance of $15\ \Omega$ at Line 6–7. Figure 5 presents the simulation results. The developed DFDI only in faulty lines and phases exceeds the threshold and both faults are properly detected by the proposed scheme.

Due to repairs or unavailability of the primary energy source of some RES units at some hours of the day, there is a possibility of these units being out of service. If this RES unit is in the end section of the feeder, the power flow in that section is

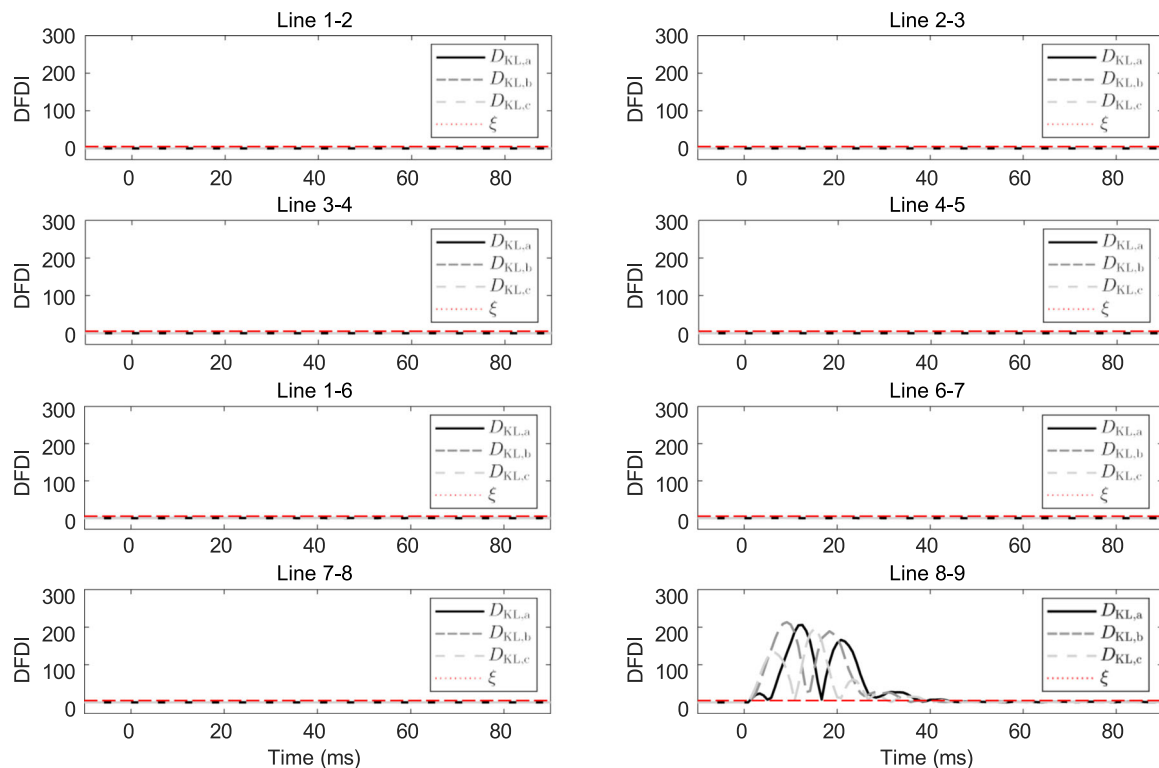


FIGURE 3 | Proposed DFDI for a severe ABCG fault condition at Line 8–9.

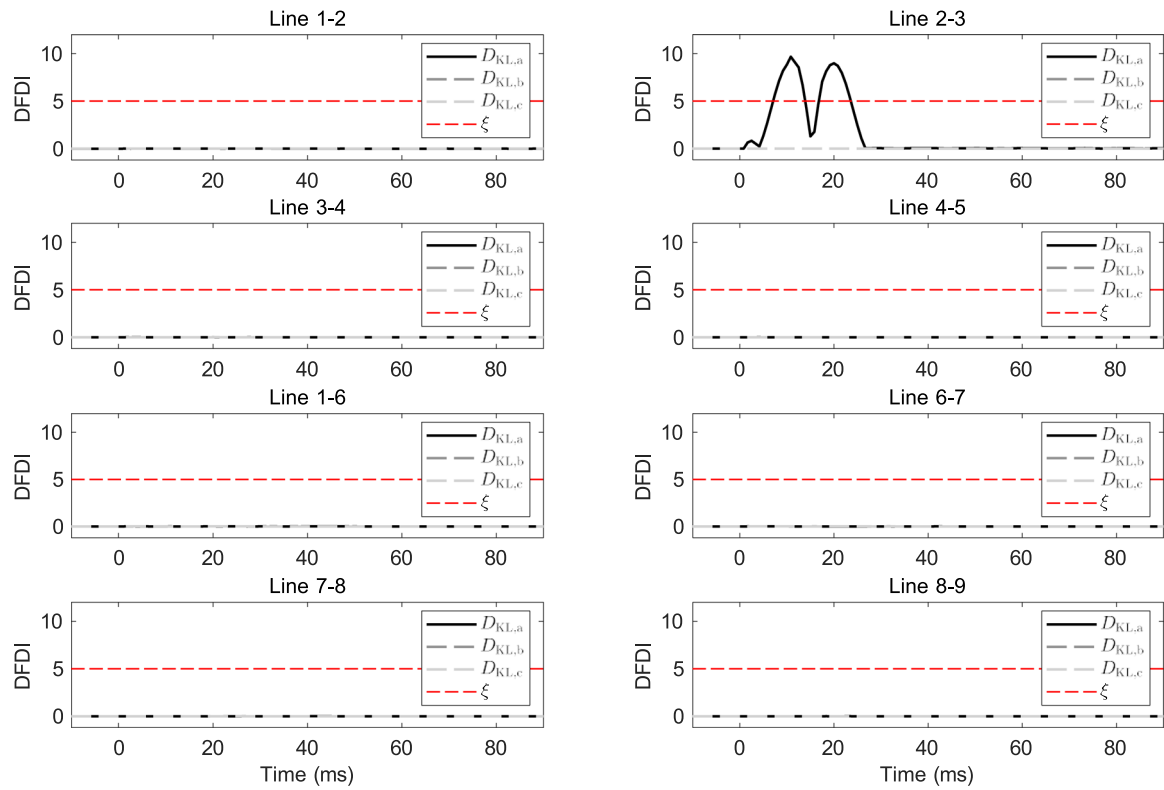


FIGURE 4 | Proposed DFDI in the case of a high resistance fault Line 2-3.

TABLE 2 | Proposed DFDI for a BC fault with various fault inception angles.

	$D_{KL,a}$			$D_{KL,b}$			$D_{KL,c}$		
	0°	45°	90°	0°	45°	90°	0°	45°	90°
Line 1-2	0	0	0	0.03	0	0.02	0.03	0	0.02
Line 2-3	0	0	0	0.01	0	0.03	0.01	0	0.03
Line 3-4	0	0	0	0.02	0	0.03	0.02	0	0.06
Line 4-5	0	0	0	131.4	143.1	139.7	130.8	143.5	14-0.1
Line 1-6	0	0	0	0.03	0	0.03	0.03	0	0.03
Line 6-7	0	0	0	0.04	0	0.03	0.04	0	0.03
Line 7-8	0	0	0	0.04	0	0.05	0.03	0	0.05
Line 8-9	0	0	0	0.03	0.01	0.06	0.03	0.01	0.06

TABLE 3 | Proposed DFDI for a BG fault in the presence of measurement noise.

	$D_{KL,a}$	$D_{KL,b}$	$D_{KL,c}$
Line 1-2	2.31	2.37	1.88
Line 2-3	2.1	2.09	1.95
Line 3-4	2.68	18.31	2.62
Line 4-5	1.93	2.32	2.23
Line 1-6	2.16	2.45	2.18
Line 6-7	2.67	2.09	2.48
Line 7-8	2.12	2	1.84
Line 8-9	2.12	1.94	2.11

TABLE 4 | Proposed DFDI for an ABCG fault in the presence of nonlinear load.

	$D_{KL,a}$	$D_{KL,b}$	$D_{KL,c}$
Line 1-2	361.66	365.88	349.76
Line 2-3	0.22	0.04	0.25
Line 3-4	0.13	0.02	0.15
Line 4-5	0.18	0.03	0.21
Line 1-6	0.15	0.04	0.19
Line 6-7	0.2	0.05	0.24
Line 7-8	0.23	0.06	0.29
Line 8-9	0.29	0.06	0.35

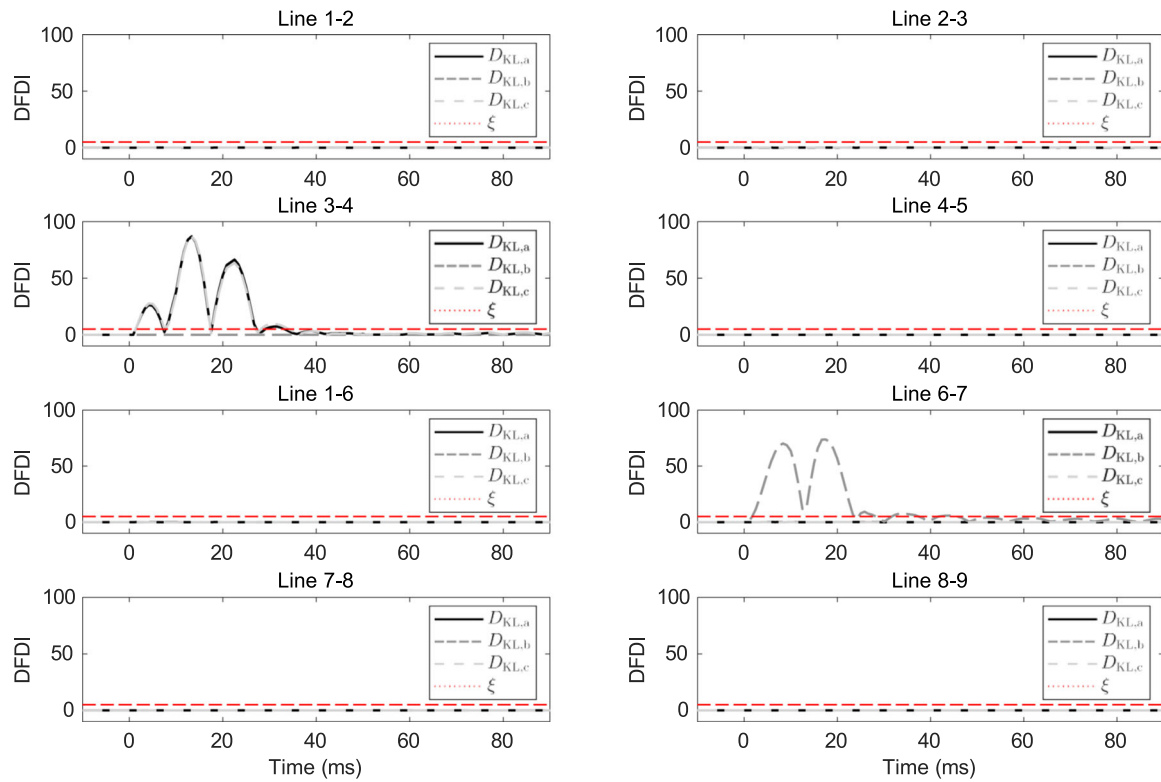


FIGURE 5 | Proposed DFDI in the case of simultaneous faults at Line 3-4 and 6-7.

TABLE 5 | Proposed DFDI for an ABCG Fault in Unidirectional Line.

	$D_{KL,a}$	$D_{KL,b}$	$D_{KL,c}$
Line 1-2	0.06	0.02	0.05
Line 2-3	0.04	0.03	0.08
Line 3-4	0.06	0.04	0.1
Line 4-5	0.03	0.02	0.04
Line 1-6	0.08	0.06	0.16
Line 6-7	0.05	0.03	0.1
Line 7-8	224.54	220.1	205.01
Line 8-9	0.45	0.36	0.79

unidirectional. To evaluate the performance of the proposed scheme for such conditions, RES4 is disconnected; also, L3, L8, and L9 are disconnected to prevent the overloading of other RES units. A solid three-phase fault is simulated at Line 7-8 which is a line with unidirectional power flow in this scenario. Table 5 presents the calculated DFDI for all lines. Only the DFDI calculated by the IED of the faulty line exceeds the fault detection threshold.

To assess the performance of the developed scheme in the case of a non-fault disturbance, the load L9 is connected to node 9; after 0.1 s, the RES2 is disconnected from node 5, and finally, after next 0.1 s, a capacitor bank for enhancing the power factor of L8 from 0.9 to 1.0 is connected to node 8. Table 6 presents the simulation results. The maximum DFDI for all lines during this simulation is near zero, verifying the secure operation of the proposed fault detection scheme.

TABLE 6 | Proposed DFDI for load, RES, and capacitor switchings.

	$D_{KL,a}$	$D_{KL,b}$	$D_{KL,c}$
Line 1-2	0.0900	0.02	0.11
Line 2-3	0.15	0.03	0.12
Line 3-4	0.05	0.01	0.06
Line 4-5	0.07	0.04	0.12
Line 1-6	0.12	0.02	0.13
Line 6-7	0.15	0.04	0.25
Line 7-8	0.16	0.06	0.13
Line 8-9	0.31	0.07	0.44

Operating mode transition represents another critical non-fault disturbance that must be thoroughly evaluated to ensure the reliability of the proposed scheme. In this scenario, the study microgrid initially operates in grid-connected mode. To simulate the transition to islanded mode, the grid interface switch S1 is opened, isolating the microgrid from the main grid. The simulation results, presented in Table 7, indicate that no mal-operation occurred in any of the IEDs. This outcome demonstrates the robustness of the proposed protection scheme when faced with non-fault disturbances.

Some microgrids are designed with loop configuration to increase the reliability of continuously supplying the loads, complicating the faulty line identification. To evaluate the performance of the proposed scheme in a microgrid with loop configuration, the switch S2 is closed and a two-phase to ground (*abg*) fault with fault resistance of $10\ \Omega$ is simulated at Line 1-6.

TABLE 7 | Proposed DFDI for operating mode change.

	$D_{KL,a}$	$D_{KL,b}$	$D_{KL,c}$
Line 1-2	0.01	0	0.01
Line 2-3	0.01	0	0.01
Line 3-4	0.01	0	0
Line 4-5	0.01	0.01	0.01
Line 1-6	0.01	0.01	0.01
Line 6-7	0.01	0.01	0
Line 7-8	0.01	0.01	0
Line 8-9	0.01	0	0.01

TABLE 8 | Proposed DFDI for an ABG Fault with Loop Configuration.

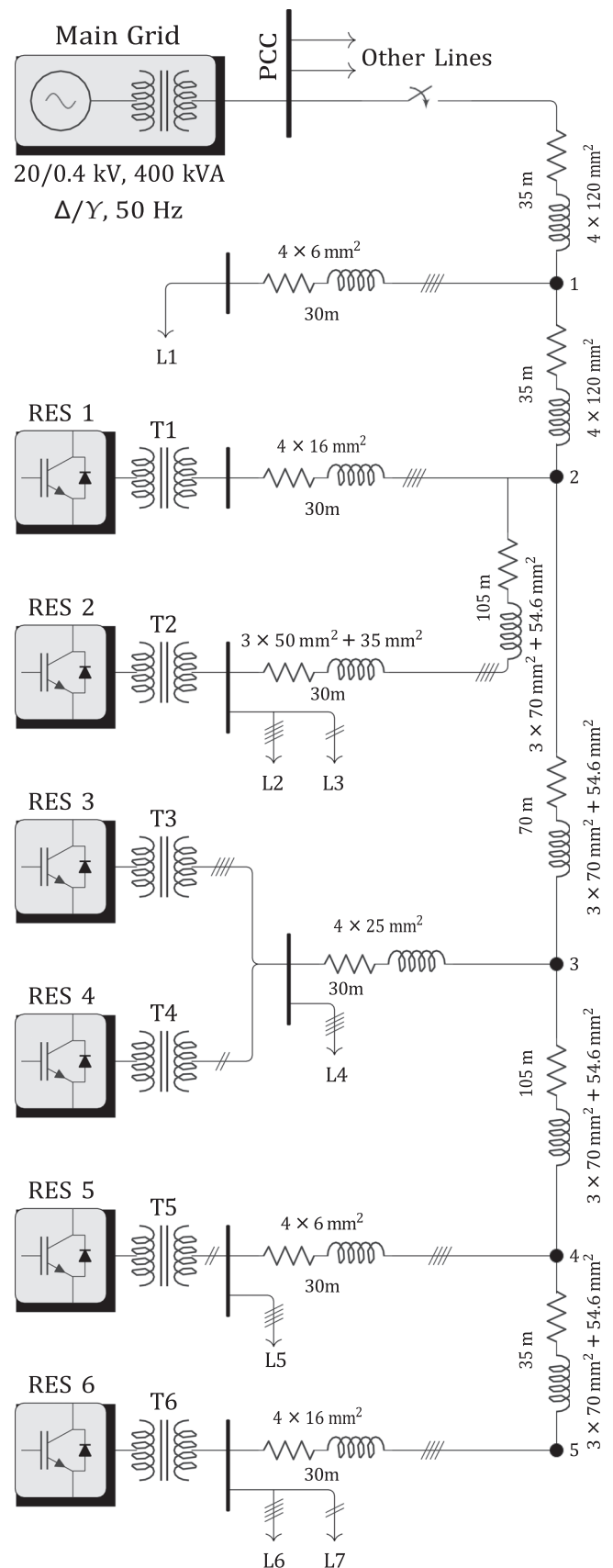
	$D_{KL,a}$	$D_{KL,b}$	$D_{KL,c}$
Line 1-2	0.01	0.01	0.02
Line 2-3	0.01	0.01	0.01
Line 3-4	0.01	0	0.01
Line 4-5	0.01	0.01	0.01
Line 1-6	44.92	55.74	0.05
Line 6-7	0.01	0.01	0.02
Line 7-8	0.01	0.01	0.01
Line 8-9	0.01	0	0.01

Table 8 presents the simulation results. The increase of the proposed DFDI only in the faulty phases of the faulty line verifies the effectiveness of the proposed scheme in microgrids with loop configuration.

To demonstrate the applicability of the proposed scheme, its performance is also evaluated in different network configurations. For this purpose, the proposed fault detection index is further evaluated in a low-voltage distribution network. The CIGRE benchmark low-voltage microgrid network [31, 32], shown in Figure 6, serves as an additional test system. This network consists of a four-wire overhead main feeder supplying a suburban residential area, with six DER units energizing the loads. Notably, Loads 3&7 and RESs 4&5 operate as single-phase units, making this system unbalanced. A solid two-phase to ground fault (*abg*) is simulated at Line 3-4. Figure 7 shows the simulation results.

The developed index is zero in all healthy lines and phases while it increases significantly in the faulty phases of Line 3-4.

Main features of the proposed fault detection scheme is compared with previous works in Figure 8. These features are: consideration of nonlinear load, capacitor switching, and operating mode transition, robustness to measurement noise and various FIAs, fault classification, and performance evaluation for high-resistance faults and various test systems. This comparison verifies the acceptable performance of the proposed scheme.

**FIGURE 6** | Single-line diagram of the CIGRE benchmark low-voltage microgrid.

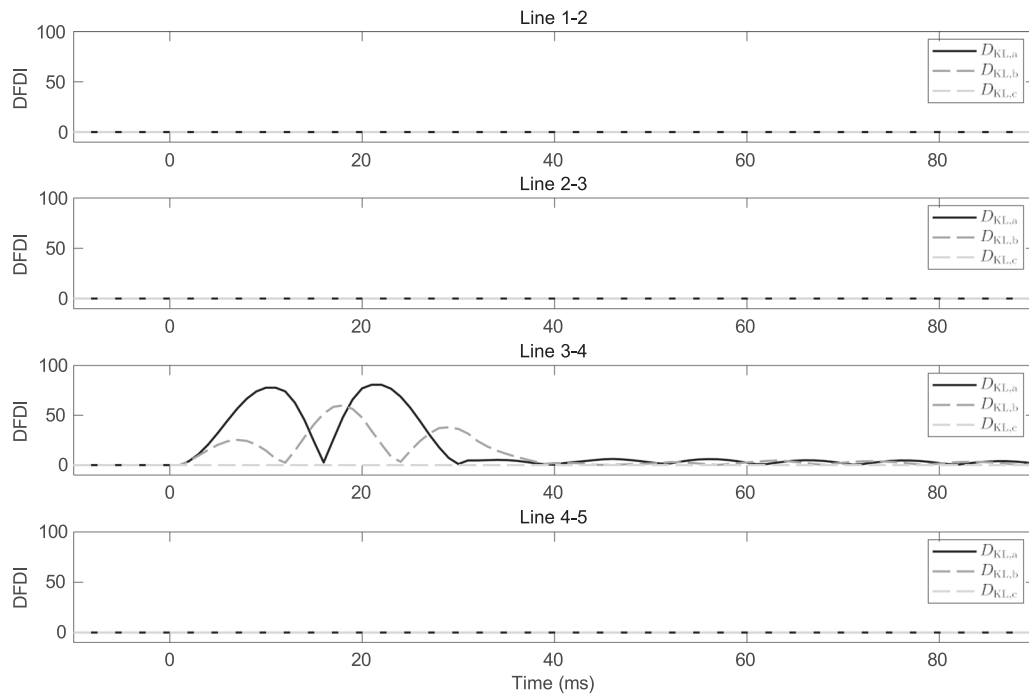


FIGURE 7 | Proposed DFDI in the case of solid *abg* fault at Line 3–4 of the CIGRE benchmark low-voltage microgrid.

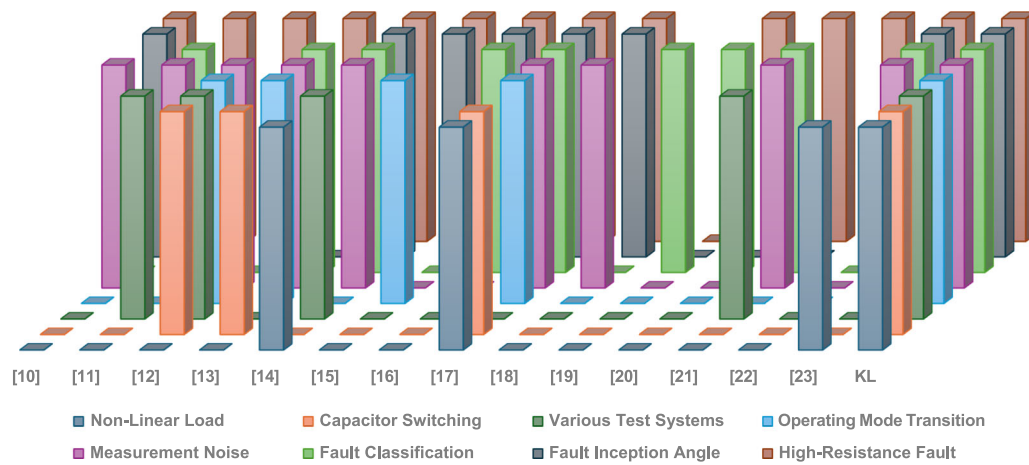


FIGURE 8 | Comparison of the proposed KL-based scheme with some existing schemes.

4 | Conclusion

To overcome the decrease in efficacy of conventional protective devices caused by the integration of RES units into modern electric energy systems, this article presents a differential fault detection scheme for 100% inverter-interfaced microgrids. The IED of each line calculates the superimposed component of line-end current signals. By using the similarity measure of KL divergence, the different changes in line-end currents of a faulty line are quantified. As verified by various simulation scenarios on two benchmark microgrids, the proposed DFDI detects various types of fault in different locations with fault resistance up to 100 Ω . No mal-operation for load, RES unit, and capacitor bank switchings as well as operating mode change verifies the security of the proposed fault detection scheme. In addition to robustness to various FIAs, the proposed DFDI properly operates in both radial and loop configurations. Moreover, it has

high immunity to harmonics and measurement noise up to 25 dB. While the fixed threshold is selected based on extensive simulations, it is acknowledged that dynamic operating conditions may warrant the exploration of adaptive or dynamic thresholding as a potential area for future work. Also, investigating the impact of cyberattacks on the proposed fault detection scheme and exploring potential mitigation strategies to enhance its resilience against such threats, as well as exploring the potential for hardware-in-the-loop testing or real-world experiments are proposed as another future work.

References

1. M. Parhamfar, I. Sadeghkhani, and A. M. Adeli, "Towards the Net Zero Carbon Future: A Review of Blockchain-Enabled Peer-to-Peer Carbon Trading," *Energy Science & Engineering* 12, no. 3 (2024): 1242–1264.

2. G. Jing, D. Wang, Q. Xiao, Q. Shen, and B. Huang, "Power Quality Disturbance Signal Classification in Microgrid Based on Kernel Extreme Learning Machine," *Electronics Letters* 60, no. 16 (2024): e13312.
3. K. Kumar, P. Kumar, and S. Kar, "A Review of Microgrid Protection for Addressing Challenges and Solutions," *Renewable Energy Focus* 49 (2024): 100572.
4. K. A and V. C, "Design of Adaptive Protection Coordination Scheme Using Svm for an AC Microgrid," *Energy Reports* 11 (2024): 4688–4712.
5. S. H. Horowitz and A. G. Phadke, *Power System Relaying*, 4th ed. (Wiley, 2014).
6. S. Ansari, O. Hari Gupta, and O. P. Malik, "Fault Detection for Microgrid Feeders Using Features Based on Superimposed Positive-Sequence Power," *Journal of Modern Power Systems and Clean Energy* 11, no. 6 (2023): 1948–1958.
7. J. Sharma and T. S. Sidhu, "A New Protection Scheme for Feeders of Microgrids With Inverter-Based Resources," *Electric Power Systems Research* 224 (2023): 109632.
8. M.-R. H. Rezaeieh, T. G. Bolandi, and S. M. Jalalat, "A Novel Approach for Resilient Protection of AC Microgrid Based on Differential Phase Angle of Superimposed Complex Power," *Sustainable Energy, Grids and Networks* 34 (2023): 101024.
9. K. Kumar and S. Kar, "An Efficient Protection Scheme for Microgrid Using ROC of Differential Admittance Angle," *Electric Power Systems Research* 227 (2024): 109969.
10. B. A. M. Alizadeh and M. F. M. Arani, "Improved Differential Based Protection Scheme for Renewable Energy Based Microgrids With Low Communication Burden," *IEEE Access* 12 (2024): 49 007–49 016.
11. S. Samal, S. R. Samantaray, and N. K. Sharma, "Data-Mining Model-Based Enhanced Differential Relaying Scheme for Microgrids," *IEEE Systems Journal* 17, no. 3 (2023): 3623–3634.
12. G. S. Dua, B. Tyagi, and V. Kumar, "Microgrid Differential Protection Based on Superimposed Current Angle Employing Synchrophasors," *IEEE Transactions on Industrial Informatics* 19, no. 8 (2023): 8775–8783.
13. A. H. N. Tajani, A. Bamshad, and N. Ghaffarzadeh, "A Novel Differential Protection Scheme for AC Microgrids Based on Discrete Wavelet Transform," *Electric Power Systems Research* 220 (2023): 109292.
14. A. Saber, H. Zeineldin, T. H. EL-Fouly, and A. Al-Durra, "A Signed Correlation Index-Based Differential Protection Scheme for Inverter-Based Islanded Microgrids," *International Journal of Electrical Power & Energy Systems* 145 (2023): 108721.
15. A. M. Joshua and K. P. Vittal, "Superimposed Current Based Differential Protection Scheme for AC Microgrid Feeders," *Applied Energy* 341 (2023): 121079.
16. A. Chandra, G. K. Singh, and V. Pant, "A Novel Protection Strategy for Microgrid Based on Estimated Differential Energy of Fault Currents," *Electric Power Systems Research* 214 (2023): 108824.
17. Z. Moravej, A. Ebrahimi, and M. Barati, "A New Differential Protection Scheme Based on Synchro-Squeezing Transform Applied to AC Micro-Grid," *Electric Power Systems Research* 231 (2024): 110336.
18. D. Liu, A. Dysko, Q. Hong, D. Tzelepis, and C. D. Booth, "Transient Wavelet Energy-Based Protection Scheme for Inverter-Dominated Microgrid," *IEEE Transactions on Smart Grid* 13, no. 4 (2022): 2533–2546.
19. A. Soleimanisardoo, H. Kazemi Karegar, and H. H. Zeineldin, "Differential Frequency Protection Scheme Based on Off-Nominal Frequency Injections for Inverter-Based Islanded Microgrids," *IEEE Transactions on Smart Grid* 10, no. 2 (2019): 2107–2114.
20. W. T. El-Sayed, E. F. El-Saadany, and H. H. Zeineldin, "Inter-harmonic Differential Relay With a Soft Current Limiter for the Protection of Inverter-Based Islanded Microgrids," *IEEE Transactions on Power Delivery* 36, no. 3 (2021): 1349–1359.
21. A. Arunan, T. Sirojan, J. Ravishankar, and E. Ambikairajah, "Real-Time Adaptive Differential Feature-Based Protection Scheme for Isolated Microgrids Using Edge Computing," *IEEE Systems Journal* 15, no. 1 (2021): 1318–1328.
22. E. Sortomme, S. S. Venkata, and J. Mitra, "Microgrid Protection Using Communication-Assisted Digital Relays," *IEEE Transactions on Power Delivery* 25, no. 4 (2010): 2789–2796.
23. A. Mallahi and I. Sadeghkhani, "A Waveform Similarity Based Current-Only Differential Protection Technique for In-Verter Interfaced Microgrids," *Electric Power Systems Research* 241 (2025): 111295.
24. A. Youssef, C. Delpha, and D. Diallo, "An Optimal Fault Detection Threshold for Early Detection Using Kullback–Leibler Divergence for Unknown Distribution Data," *Signal processing* 120 (2016): 266–279.
25. H. Chen, B. Jiang, and N. Lu, "An Improved Incipient Fault Detection Method Based on Kullback-Leibler Divergence," *ISA Transactions* 79 (2018): 127–136.
26. J. Harmouche, C. Delpha, and D. Diallo, "Incipient Fault Detection and Diagnosis Based on Kullback–Leibler Divergence Using Principal Component Analysis: Part I," *Signal processing* 94 (2014): 278–287.
27. M. A. Zamani, A. Yazdani, and T. S. Sidhu, "A Communication-Assisted Protection Strategy for Inverter-Based Medium- Voltage Microgrids," *IEEE Transactions on Smart Grid* 3, no. 4 (December 2012): 2088–2099.
28. G. Benmouy and J. Roberts, "Superimposed quantities: Their True Nature and Application in Relays," in *26th Annual Western Protective Relay Conference*, Spokane, Washington, October (1999).
29. K. Dubey and P. Jena, "Impedance Angle-Based Differential Protection Scheme for Microgrid Feeders," *IEEE Systems Journal* 15, no. 3 (2021): 3291–3300.
30. W. K. A. Najy, H. H. Zeineldin, and W. L. Woon, "Optimal Protection Coordination for Microgrids With Grid-Connected and Islanded Capability," *IEEE Transactions on Industrial Electronics* 60, no. 4 (2013): 1668–1677.
31. I. Sadeghkhani, M. E. Hamedani Golshan, A. Mehrizi-Sani, J. M. Guerrero, and A. Ketabi, "Transient Monitoring Function-Based Fault Detection for Inverter-Interfaced Microgrids," *IEEE Transactions on Smart Grid* 9, no. 3 (2018): 2097–2107.
32. S. Papathanassiou, N. Hatziaargyriou, and K. Strunz, "A Benchmark Low Voltage Microgrid Network," in *CIGRE Symposium on Power Systems With Dispersed Generation*, Athens, Greece, April (2005).